



Thermoresponsive and antibacterial two-dimensional polyglycerol-*interlocked*-polynipam for targeted drug delivery

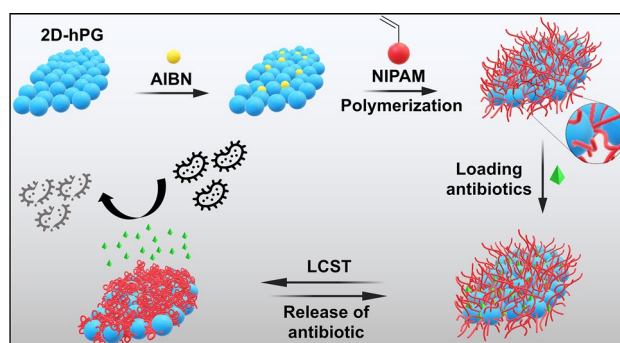
Nasim Khosravani¹ · Vahid Ahmadi² · Ali Kakanejadifard¹ · Mohsen Adeli¹

Received: 26 May 2022 / Revised: 5 September 2022 / Accepted: 6 September 2022 / Published online: 30 September 2022
© The Author(s), under exclusive licence to Islamic Azad University 2022

Abstract

Two-dimensional polymeric networks are a new class of polymers with interesting physicochemical and biological properties. They promise a wide range of future biomedical applications including pathogen interactions, drug delivery, bioimaging, photothermal, and photodynamic therapy, owing to their unique features, such as high surface area and multivalent interactions at nano-biointerfaces. In this work, a thermosensitive two-dimensional polymeric network consisting poly(*N*-isopropylacrylamide) (pNIPAM) chains that are mechanically interlocked by a polyglycerol platform was synthesized and used for bacteria incapacitation. Two-dimensional hyperbranched polyglycerol (2D-hPG) was synthesized by a graphene-assisted strategy and used for encapsulation of azobisisobutyronitrile (AIBN). Radical polymerization of *N*-isopropylacrylamide by encapsulated AIBN resulted in thermoresponsive platforms with ~ 500 nm lateral size and 20–50 nm thickness. Due to its porous structure, 2D-PNPG was able to efficiently load antibiotics, such as tetracycline (TC) and amoxicillin (AMX). The rate of release of antibiotics from 2D-PNPG and the antibacterial activity of the system correlated with the variation of temperature as a result of the thermosensitivity of 2D-PNPG. This study shows that two-dimensional polymers are efficient platforms for future biomedical applications including drug delivery and bacteria incapacitation.

Graphical abstract



Thermoresponsive two-dimensional nanomaterials with the ability of loading therapeutic agents and antibacterial activity are synthesized and characterized.

Keywords Antibacterial · Two-dimensional · Polyglycerol · Thermoresponsive · *N*-isopropylacrylamide

✉ Mohsen Adeli
mohadeli@yahoo.com; adeli.m@lu.ac.ir

¹ Department of Chemistry, Faculty of Science, Lorestan University, Khoramabad 68151-44316, Iran

² Institut für Chemie und Biochemie, Freie Universität Berlin, Takustrasse 3, 14195 Berlin, Germany

Introduction

Infectious diseases are endangering human health, and the discovery of new ways to treat these infectious diseases has attracted worldwide attention. Exploring new materials with antibacterial activity has become one of the most urgent



topics in the last two decades, as it negatively impacts public health worldwide [1–14]. The long-term and excessive use of antibiotics to treat these infectious diseases has caused the spread drug-resistant bacteria. Moreover, some of therapeutic agents degraded into inactive materials before getting into the target site, decreasing their efficiency and activity against infections and bacteria dramatically. Therefore, the development of smart systems to support and transport antibiotics has received high attention in the past decade. Smart antibacterial systems with the ability of specific interactions with bacteria induce fewer side effects and toxicity against human cells [15–22]. Stimuli-responsive polymers have attracted a great deal of attention in chromatography, biomedicine, and bioengineering, due to their ability to respond to various stimuli factors including pH, temperature, ionic strength, redox reactions, light, shear stress, and enzymes [23–26]. Among the stimuli-responsive polymers, thermoresponsive polymers have been intensively used for different biomedical applications. Poly(*N*-isopropylacrylamide) (pNIPAM) is a thermoresponsive linear polymer with a flexible, sponge-like structure and a lower critical solution temperature (LCST) of about 32 °C in water [27–31]. As a result of such features, this polymer has emerged as an attractive candidate for various medical applications ranging from drug delivery to bacterial interactions [32–34]. Moreover, this polymer has been successfully employed in the fabrication of a wide range of materials including hydrogels [35], nanoparticles [36], nanofibrous [29], etc. A recent study has shown a strong correlation between morphology and antibacterial activity of this polymer [29].

Recently, two-dimensional nanomaterials (2DNs) have received much attention due to their exceptional properties and potential applications. 2DNs with flat topology and high surface area are interesting materials for different biomedical applications [1–3, 37–40]. Due to their sheet-like structure, and accessible functional groups, they can strongly interact with pathogens and destroy them by different mechanisms [4, 5, 7, 41–43]. We have shown that morphology, functionality, and hydrophobicity are important factors, dominating interactions of these materials at nano-biointerfaces [2, 4, 32, 44]. Recently, we have implemented a new method for the construction of two-dimensional polyglycerols (2D-hPG) using a graphene template via Cu(I)-catalyzed click reaction [44]. The sulfated version of 2D-hPG, as a heparan mimic compound, showed an IC₅₀ value of 3 nm for inhibition of SARS-CoV-2 [45, 46]. The strong virus interaction and low IC₅₀ of this compound were assigned to the high surface area and accessible negatively charged functional groups. Hydrophobic interactions are one of the main driving forces for the incapacitation of viruses and bacteria [4, 32, 42, 47]. To boost the antibacterial activity of 2D-hPG with hydrophobic forces, *N*-isopropylacrylamide was polymerized inside the pores of this compound, and two-dimensional

pNIPAM-*interlocked*-polyglycerol was obtained. Different spectroscopy and microscopy analyses showed that pNIPAM chains were entangled with 2D-hPG platform, inducing a thermosensitivity for the whole system. The obtained thermoresponsive two-dimensional compound was able to load antibiotics. A change in the temperature of the medium triggered the release of loaded antibiotics and resulted in antibacterial activity.

Experimental

Materials

N-isopropylacrylamide (NIPAM), tetracycline (TC), and amoxicillin (AMX) were purchased from Sigma-Aldrich. Azobisisobutyronitrile (AIBN) and methanol (99.9%) were provided by Merck and used without further purification. Dialysis bag 100 kDa, 14 kDa and 2 kDa cutoff was provided by spectrum company. *E. coli* strain (*E. coli*) (PTCC 1330) and *staphylococcus aureus* (*S. aureus*) (PTCC 1112), were obtained from the Pasteur Institute, Tehran–Iran.

Methods and instrumentations

IR spectra of the synthesized materials were obtained by FT-IR spectrometer (Tensor 320, Bruker, Germany) at ambient conditions and in 4000–400 cm⁻¹ range using KBr pellet at a weight ratio of 5/200 mg. The size and morphologies of materials were investigated by dropping a solution of materials on silica substrate and recording image by LEO 440i scanning electron microscope (FESEM, Tescan, Czech) equipped with energy dispersive X-ray spectrometer (EDX) under at 10 kV. Composition of materials, elemental analysis (CHNS), was investigated by an CHNS apparatus (ECS 4010, NC technologies (Costech), Italy) with detectors for carbon, hydrogen, and nitrogen. Proton nuclear magnetic resonance (¹H NMR) spectra were obtained using a 400 MHz NMR spectrometer (Avance 400MHz, Bruker, Germany). AFM images were recorded using a AFM apparatus (full plus, ARA–AFM, Iran), operated in tapping mode.

Synthetic procedures

Sample preparation for SEM at 25 °C and 40 °C

An aqueous dispersion of 2D-PNPG, 2D-PNPG₁₄ and 2D-PNPG₃₀₀ (0.1 mg/ml) was dropped on a lamellar surface and dried at two different temperatures (25 °C and 40 °C). Then, they were coated with a thin layer of gold by sputtering for 15 s.

Sample preparation for AFM at 25 °C and 40 °C

An aqueous dispersion of 2D-PNPG₁₄ and 2D-PNPG₃₀₀ (0.1 mg/ml) was dropped on a mica substrate and solvent was evaporated at two different temperatures (25 °C and 40 °C). Measurements were performed using a full plus AFM apparatus, operated in tapping mode.

Synthesis of two-dimensional polyglycerol (2D-hPG)

Two-dimensional polyglycerol (2D-hPG) was prepared according to our previously reported procedure in literature [44]. Briefly, hyperbranched polyglycerol with ~10% azide functional groups (hPG-N₃) was covalently attached to the surface of reduced graphene oxide containing acetal dichlorotriazine functional groups (G-Trz) through pH-sensitive linkers. Tripropargylamine was then loaded onto the surface of polyglycerol-functionalized graphene and moved toward azide functional groups for a lateral crosslinking via Cu(I)-catalyzed click chemistry. Afterward, polyglycerol sheets were separated from the surface by acidification and centrifugation.

Synthesis of two-dimensional poly(N-isopropylacrylamide)-interlocked-polyglycerol (2D-PNPG)

2D-hPG (200 mg) was dissolved in water (3 ml) and the obtained solution was stirred for 30 min at room temperature. AIBN (2 g, 12.179 mmol) was added to this solution in a 100 ml round-bottom flask and mixture was stirred at room temperature for 48 h to incorporate the initiator into the 2D-hPG pores. Free AIBN was removed by filtering and centrifugation at 2000 rpm for 10 min three times. N-isopropylacrylamide was added to this solution and stirred at 75 °C for 10–12 h. The reaction mixture was cooled down and product was precipitated by addition of MeOH. The obtained product was dialyzed (14 kDa cutoff) against water/methanol for 1 day at room temperature and stored in fridge. 2D-PNPG with different compositions were synthesized using 14/1 and 300/1 w/w ratios of NIPAM/2D-hPG.

Loading and release of antibiotics by 2D-PNPG

2D-PNPG (0.1 g) was dispersed in PBS by sonication. Then, tetracycline and amoxicillin (0.05 g) were added to the obtained dispersion slowly and mixture was stirred at 27 °C for 24 h. The obtained product was dialyzed (2 kDa cutoff) against water/ethanol and purified. The drug loading efficiency of the 2D-PNPG was calculated using the following equations:

Drug loading efficiency

$$= \frac{\text{amount of a drug in the nanoparticle}}{\text{total amount of drug applied in the formulation}}$$

The release of antibiotics from 2D nanomaterials was evaluated using a dialysis bag (2 kDa) in PBS with pH 7.4 at 27 °C and 37 °C. 2D-PNPG/antibiotic (10 mg) in PBS (5 ml) was added to a dialysis bag and it was incubated in a beaker containing PBS (20 ml) at 27 °C and 37 °C. At specific time intervals, a part of the outer solution of the dialysis bag (2.5 ml) was taken out and its UV absorption was measured and then returned to the medium. The concentration of the released drug was calculated by measuring the UV absorption of excluded solution using a calibration curve.

Antibacterial activities

Antibacterial activity of 2D nanomaterials was tested against *Staphylococcus aureus* (*S. aureus*) and *Escherichia coli* (*E. coli*) bacteria by agar diffusion assay. Bacteria were cultured on nutrient agar plates and inoculated for 24 h. The suspension of bacterial was diluted using PBS to 1.5×10^8 CFU/ml. Afterward, the suspension of bacteria (100 µl) was added on agar and the aqueous solution of the samples (192, 96, and 48) µg/disc was poured on the surface of the discs and the discs were placed on the plates at 27 °C and 37 °C for 24 h. The tetracycline and amoxicillin (48 µg/disc) were used as positive control and distilled water was considered as negative control in antibacterial tests. Finally, the bacterial growth in the plates was evaluated by measuring the inhibition zone.

Results and discussion

2D polyglycerol was synthesized according to our reported procedure in literature [41] and used for the construction of thermosensitive two-dimensional polymeric networks consisting pNIPAM chains interlocked by this platform (Fig. 1b). 2D-hPG was constructed using a graphene-assisted and copper(I)-catalyzed click strategy (Fig. 1a). The porous structure of in aqueous solution. Initiating and propagating pNIPAM chains inside porous 2D-hPG resulted in thermosensitive two-dimensional networks with the ability of loading therapeutic agents. The mass ratio of pNIPAM inside 2D-hPG was adjusted using different mass ratios of NIPAM monomer to two-dimensional polyglycerol (NIPAM/2D-hPG). NIPAM/2D-hPG ratios of 14/1 and 300/1 resulted in two products called 2D-PNPG₁₄ and 2D-PNPG₃₀₀, respectively. The 2D-PNPG₁₄ with short pNIPAM chains was synthesized to enable us to detect signals of both 2D-hPG and pNIPAM components in the ¹H NMR spectrum for an easy characterization and monitoring the synthesis process (Fig. 2B).

2D-PNPG₃₀₀ with the long pNIPAM chains was synthesized to improve the thermosensitivity of the platform and



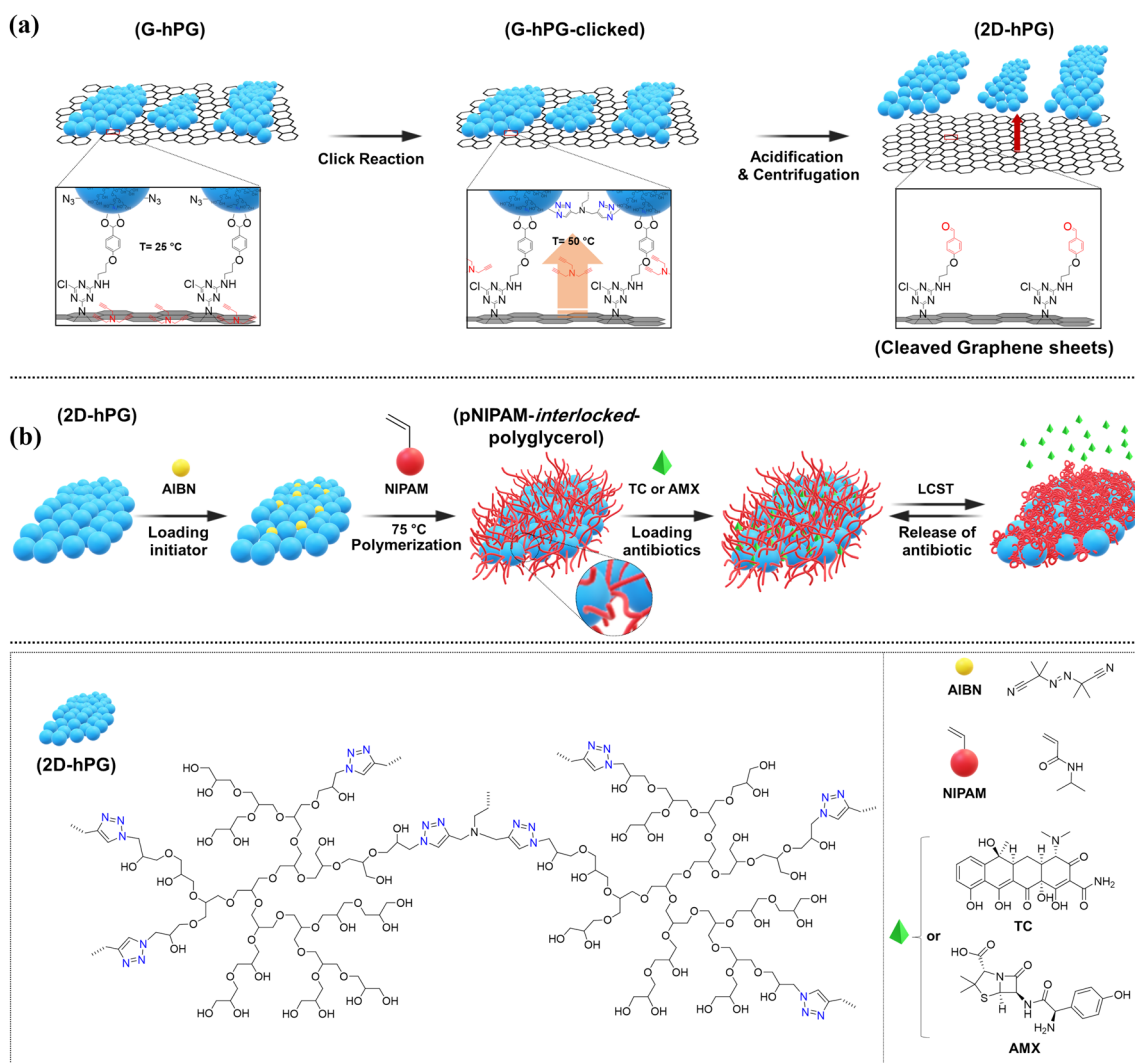


Fig. 1 **a** Schematic representation of the reaction process for the preparation of 2D-hPG. 2D-hPG was synthesized using a graphene-assisted and copper(I)-catalyzed click reaction. **b** Synthesis of two-

dimensional polymeric networks consisting pNIPAM chains interlocked by polyglycerol platform and finally loading and release of (TC) and (AMX) at lower critical solution temperature (LCST)

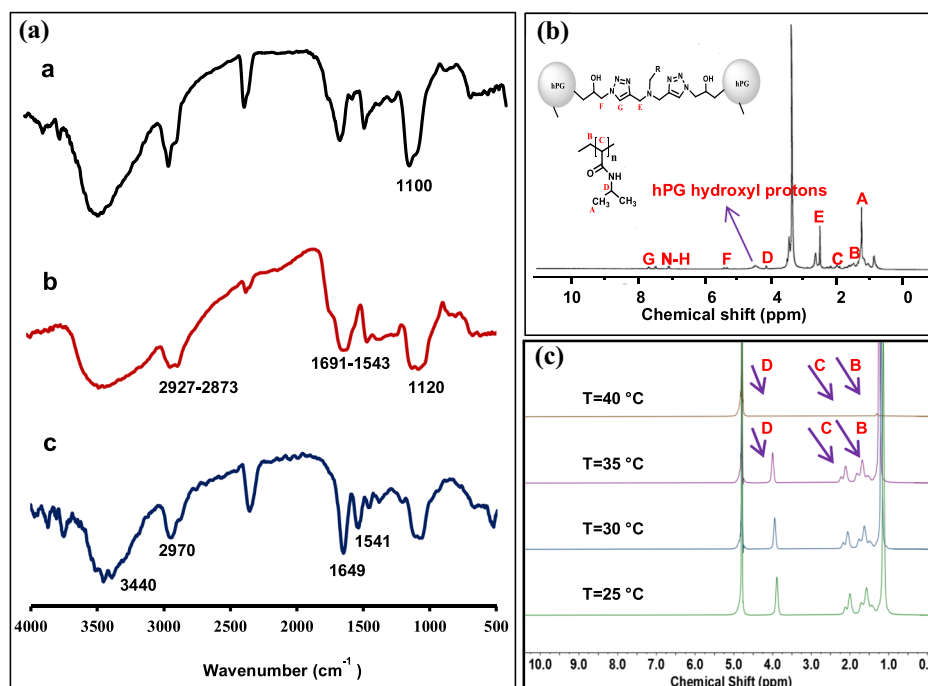
manipulate its hydrophilicity for drug release and bacterial interactions.

The synthesized two-dimensional nanomaterials were characterized using different spectroscopy and microscopy methods. IR spectrum of 2D-hPG displays absorbance bands at 1100 cm^{-1} , 2900 cm^{-1} , and 3400 cm^{-1} corresponding to C–O, aliphatic C–H, and hydroxyl functional groups of polyglycerol, respectively (Fig. 2Aa) [44]. After polymerization of NIPAM monomer by encapsulated AIBN, absorbance bands of carbonyl groups of pNIPAM were appeared at 1649 cm^{-1} (Fig. 2Ab). In the IR spectrum of 2D-PNPG₃₀₀, absorbance bands at 3440 cm^{-1} , 2970 cm^{-1} , 2860 cm^{-1} , and 1649 cm^{-1} were corresponding to N–H, CH₃, CH₂, and carbonyl groups of pNIPAM chains, respectively (Fig. 2Ac). These absorbance bands indicated successful polymerization of NIPAM monomer inside pores of 2D-hPG. The ¹H

NMR spectrum of 2D-PNPG₁₄ exhibited signals of protons of pNIPAM chains at 4.16–4.11 ppm (NHCH(CH₃)₂), 1.27–1.23 ppm (CH₃), 1.70–1.46 ppm (–CH₂CH₃), 2.18–1.90 ppm (–CH–), 2.53–2.49 ppm and 7.12–7.06 ppm (NH–) (Fig. 2B). In addition, signals at 3.83–3.49 ppm corresponding to protons of polyglycerol and signals at 5.40–5.31 ppm and 7.70–7.67 ppm related to protons of methylene group and triazole ring, respectively, confirming the successful synthesis of this compound (Fig. 2B) [32].

In the ¹H NMR spectrum of 2D-PNPG₃₀₀, signals related to the 2D-hPG platform were not observed due to the thick pNIPAM shell. However, signals of pNIPAM segment were detected at 4.16–4.11 ppm (NHCH(CH₃)₂), 1.27–1.23 ppm (CH₃), 1.70–1.46 ppm (–CH₂CH₃), and 2.18–1.90 ppm (–CH–)(Fig. 2C). To explore the thermoresponsive behavior and LCST of 2D-PNPG₃₀₀, ¹H NMR spectra were recorded

Fig. 2 A IR spectra of **a** 2D-hPG, **b** 2D-PNPG₁₄ and **c** 2D-PNPG₃₀₀. ¹H NMR spectra of **B** 2D-PNPG₁₄ and **C** 2D-PNPG₃₀₀ at different temperatures (25–40 °C). While signals of pNIPAM were slightly broadened from 25 to 35 °C, they disappeared at 40 °C, indicating LCST for this compound at this range of temperature



at different temperatures. Signals of pNIPAM chains were slightly broadened at 25–35 °C and disappeared at 40 °C (Fig. 2C). This experiment indicated LCST between 35 and 40 °C and our ability to switch between hydrophobic and hydrophilic states by changing the temperature[32].

The morphology and size of 2D nanomaterials were investigated by scanning electron microscopy (SEM) and atomic force microscopy (AFM). SEM images of 2D-hPG demonstrated sheet-like structures with an average size of 200–500 nm at 25 °C and 40 °C (Fig. 3a–d). After polymerization of NIPAM within the pores of 2D-hPG, the obtained materials showed sheet-like morphologies similar to 2D-hPG platform. The SEM images recorded after increasing temperature (Fig. 3e–l) did not indicate a significant changes in the morphology and lateral sizes of 2D-PNPG₁₄ and 2D-PNPG₃₀₀.

However, in some cases and upon increasing the concentration agglomerations were observed at 40 °C. AFM images showed flat topologies with 20 and 50 nm thickness for 2D-PNPG₁₄ and 2D-PNPG₃₀₀ at 25 °C, respectively (Fig. 4a, c). When temperature of solution was increased to 40 °C, AFM showed agglomerations with 90 and 200 nm height for 2D-PNPG₁₄ and 2D-PNPG₃₀₀, respectively (Fig. 4b, d). Agglomeration of two-dimensional nanomaterials upon increasing the temperature was another indicator for their thermoresponsive property (Fig. 4a–d).

It is well-known that pNIPAM is a thermosensitive polymer and it collapses at higher than lower critical solution temperature (LCST). Figure 4e shows the temperature-dependent transmittance of 2D-PNPG₃₀₀ in water.

2D-PNPG₃₀₀ showed LCST around 32 °C. The transparent 2D-PNPG₃₀₀ aqueous solution gradually becomes opaque with increasing temperature. The color of the 2D-PNPG₃₀₀ aqueous solution became quite opaque near 35 °C. This is a simple method to measure the thermosensitive behavior of pNIPAM and its derivatives.

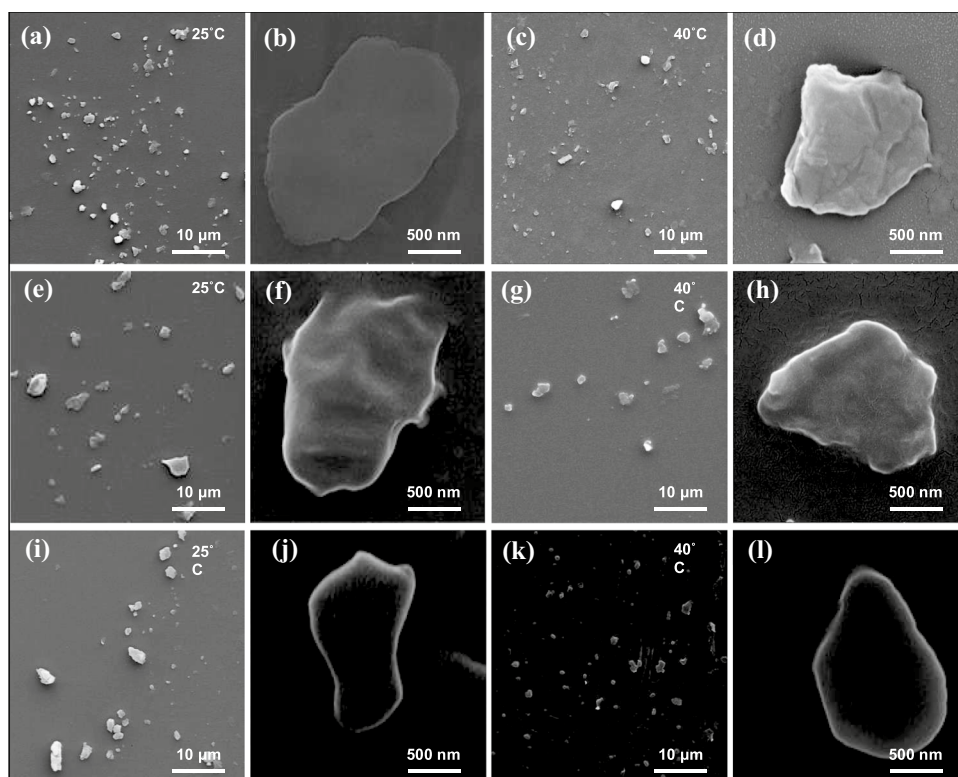
The composition of two-dimensional nanomaterials was investigated by Energy Dispersive X-Ray Analysis (EDX) and elemental analysis (Tables 1 and 2). The carbon and nitrogen content of 2D-PNPG₃₀₀ was significantly increased in comparison with 2D-hPG. Moreover, the oxygen content of 2D-hPG significantly decreased upon polymerization of NIPAM monomers. These results indicated the production of pNIPAM chains inside pores of 2D-hPG and creation of a two-dimensional nanomaterial with physically crosslinked segments.

To demonstrate the suitability of thermosensitive two-dimensional polymeric networks for drug delivery applications, amoxicillin (AMX) (Fig. 5e) and tetracycline (TC) (Fig. 5f) were loaded in their pores and the rate of their release at 27 °C and 37 °C was studied.

Using the drug loading efficiency equation, the loading efficiency of 2D-PNPG₃₀₀ for AMX and TC was found to be 70 wt% and 80 wt%, respectively.

The high loading efficiency of 2D-PNPG₃₀₀ is attributed to its porosity and high surface area. In vitro release experiment was conducted in PBS solution at pH 7.4 for 24 h to assess the drug release behavior of 2D-PNPG₃₀₀ scaffolds. temperature, 37 °C, The release rate of both

Fig. 3 SEM images at two sizes of 10 μm and 500 nm of **a–d** 2D-hPG, **e–h** 2D-PNPG₁₄ and **i–l** 2D-PNPG₃₀₀ at 25 °C and 40 °C. Samples were prepared by dropping an aqueous dispersion of materials (0.1 mg/ml) onto the lamellar surface and then drying at two different temperatures (25 °C and 40 °C). No significant changes in the morphology of two-dimensional materials were observed upon increasing the temperature



drugs AMX and TC was higher at 37 °C, above the LCST of 2D-PNPG₃₀₀, than that at 27 °C.

This is because, at 27 °C, below the LCST of 2D-PNPG₃₀₀, the pNIPAM chains are in a hydrophilic state, and pores of the two-dimensional platform are accessible to host drugs. The pNIPAM chains, however, switch to a hydrophobic state at 37 °C and collapse into the pores of the polyglycerol platform, subsequently causing the loaded drugs to be released (Fig. 5a, b). This temperature-dependent cargo release was more pronounced for AMX than TC. This can be assigned to the more hydrophilic structure of AMX, forcing it to stay inside the hydrophilic pores of the platform at low temperatures. In the case of TC with a hydrophobic structure, no significant interactions can occur between this drug and the hydrophilic pores of the platform and it cannot be associated with the system strongly. Taking advantage of this property, this compound can be potentially used to load and release therapeutic agents in biological systems (Fig. 1b).

The bacterial inhibition efficacy of the drug-loaded 2D-PNPG₃₀₀ was evaluated by qualitative analysis using a disk diffusion method. The antibacterial activity of produced polymers was tested at 27 °C and 37 °C after 24 h incubation with Gram-negative *Escherichia coli* (*E. coli*) and Gram-positive *Staphylococcus aureus* (*S. aureus*) bacteria. As shown in Figs. 5c, d, and 6a, no inhibition of the bacterial growth by 2D-PNPG₃₀₀ was observed at both temperatures and for both bacteria.

A slight antibacterial activity against *E. coli* can be assigned to mechanical stress from two-dimensional material. Any significant effect for AMX against *E. coli*, due to drug resistance effect, was not observed (Figs. 5c and 6b). Although, AMX/2D-PNPG₃₀₀ did not show temperature-dependent antibacterial activity against *E. coli*. 2D-PNPG₃₀₀ loaded with tetracycline (TC/2D-PNPG₃₀₀) showed an efficient antibacterial activity against *E. coli* at both temperatures (Figs. 5c and 6c). Considering the slightly higher level of inhibition of bacteria at 27 °C compared with 37 °C, and that the inhibition of bacteria does not increase with increasing the temperature, this can be indicate that TC is efficiently released at both temperatures (Fig. 5c). Results showed that 40 wt.% release of the loaded TC at room temperature is enough to inhibit *E. coli* efficiently. Incubation of TC/2D-PNPG₃₀₀ with *S. aureus* at 37 °C showed a good inhibition zone, which was significantly higher than that at room temperature (Figs. 5d and 6c). This can be due to a synergistic effect of the hydrophobic effect and drug release at this temperature. It is worth noting that TC/2D-PNPG₃₀₀ with a low temperature-dependent release of cargo showed different activities against Gram-positive and Gram-negative bacteria. A key reason for this is the differences in the structures of these types of bacteria, particularly their membranes, and their resistance to therapeutic agents. Incubation of AMX/2D-PNPG₃₀₀ with *S. aureus* at 27 °C did not inhibit the bacteria growth but an efficient antibacterial activity

Fig. 4 a–d and the inset of a–d are AFM images and the height profiles of a, b 2D-PNPG₁₄ and c, d 2D-PNPG₃₀₀ on mica at 25 °C and 40 °C. While individual sheets were observed at 25 °C, they were agglomerated at 40 °C due to crossing LCST of system and changing to hydrophobic state. e The photograph of thermosensitive behavior of the 2D-PNPG₃₀₀

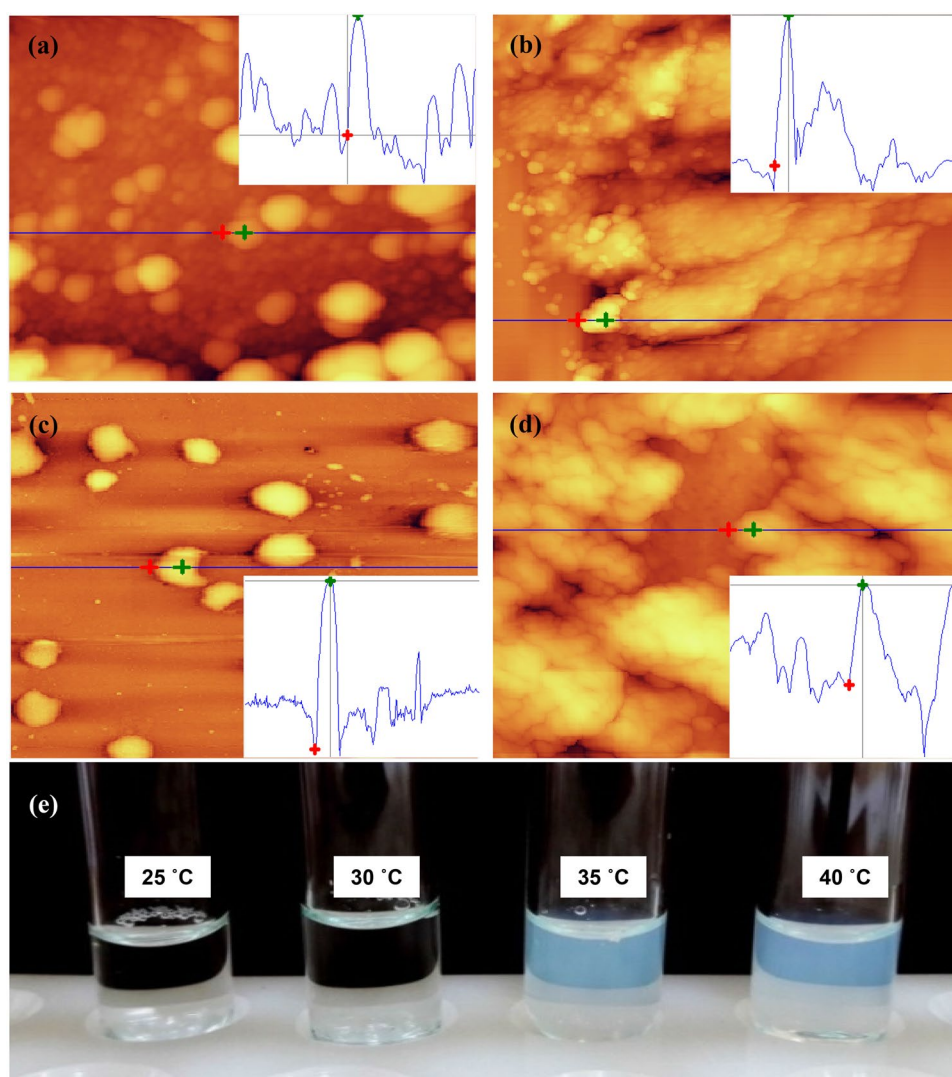


Table 1 EDX analysis of 2D-hPG, 2D-PNPG14, and 2D-PNPG300

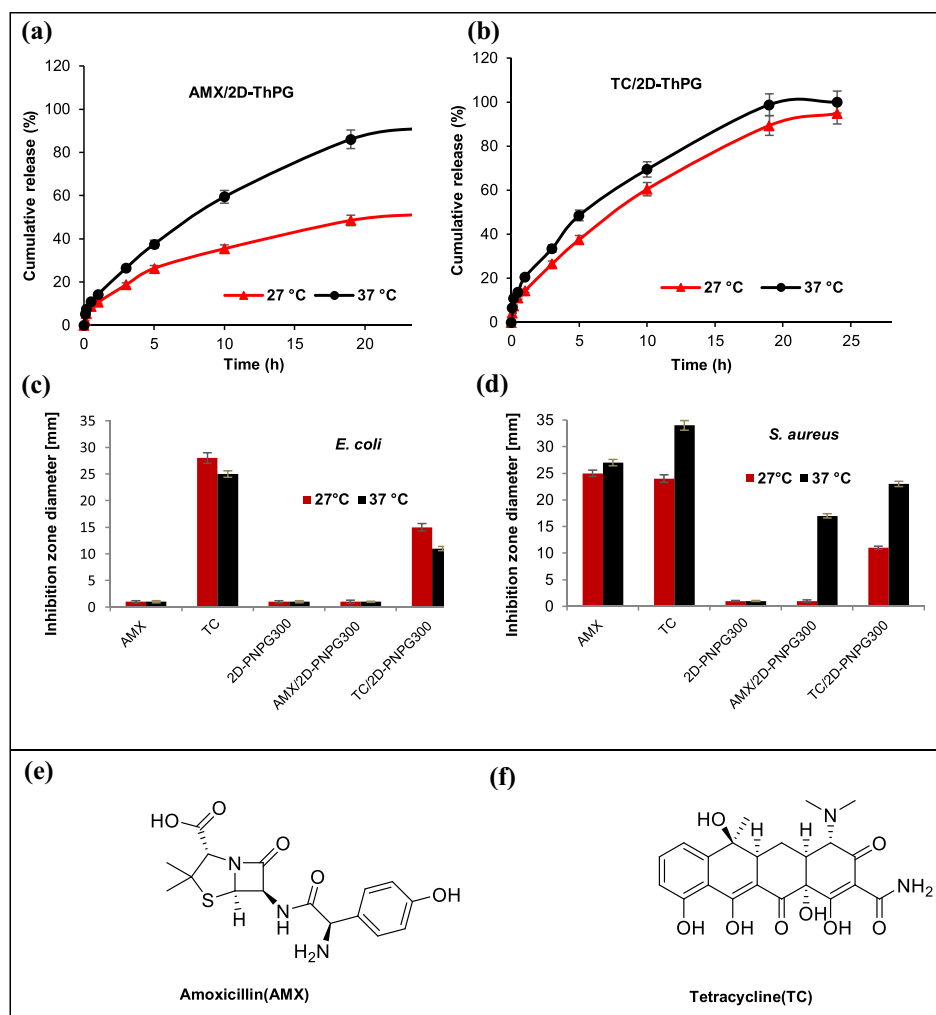
| Compound | C [wt. %] | O [wt. %] | N [wt. %] |
|------------------------|-----------|-----------|-----------|
| 2D-hPG | 48.84 | 32.04 | 19.12 |
| 2D-PNPG ₁₄ | 53.13 | 30.23 | 16.16 |
| 2D-PNPG ₃₀₀ | 61.19 | 17.04 | 21.77 |

Table 2 Elemental analysis of 2D-hPG, 2D-PNPG14, and 2D-PNPG300

| Compound | C [wt. %] | H [wt. %] | N [wt. %] |
|------------------------|-----------|-----------|-----------|
| 2D-hPG | 43.35 | 5.31 | 12.85 |
| 2D-PNPG ₁₄ | 47.30 | 6.39 | 3.99 |
| 2D-PNPG ₃₀₀ | 59.85 | 14.34 | 13.85 |

was observed upon switching to 37 °C. The higher activity of AMX/2D-PNPG₃₀₀ against *S. aureus* at a higher temperature is assigned to the efficient release of AMX at this temperature (Figs. 5c and 6b). In general, AMX/2D-PNPG₃₀₀ was more efficient and showed greater temperature-dependent activity when compared with its counterpart bearing TC drug (Figs. 5 and 6). To demonstrate the interactions between AMX/2D-PNPG₃₀₀ and *S. aureus*, this compound was incubated with this bacterium at 37 °C for 24 h. The results revealed considerable inhibition at this temperature (Fig. 6d). Regardless of the type of loaded drug, the prepared systems did not show a temperature-dependent activity against *E. coli*. Antibacterial data at a concentration of 48 µg/disc are shown in Table 3. The concentration of the drug-loaded 2D-PNPG₃₀₀ used in the antibacterial did not show significant effect on the zone inhibition of bacteria. Therefore, only 48 µg/disc was

Fig. 5 In vitro release profiles of **a** AMX from 2D-PNPG₃₀₀, and **b** TC from 2D-PNPG₃₀₀ at 27 °C and 37 °C. The release of drugs from two-dimensional materials showed a temperature-dependence behavior. This was more effective for AMX than TC. Antibacterial activity as a function of the zone of inhibition upon incubation of AMX/2D-PNPG₃₀₀ and TC/2D-PNPG₃₀₀ at a concentration of 48 µg/disc at 27 °C and 37 °C with **c** *S. aureus* and **d** *E. coli* bacteria. **e** Chemical structure of amoxicillin (AMX) and **f** tetracycline (TC)



considered. The antibacterial experiments showed that different parameters including type of drug, type of bacteria, and temperature affect the antibacterial activity of the drug-loaded two-dimensional platforms.

The controlled release of therapeutic agents together with high loading capacity and thermosensitivity of the synthesized platforms suggest them as new candidates for a wide range of biomedical applications ranging from drug delivery to tissue engineering and antibacterial activity. Intrinsic mechanical and chemical properties of two-dimensional nanomaterials, which is of high interest for the regenerative medicine, combined with the manipulated hydrophilicity can be formulated into a new vector in this field [48].

Conclusions

Thermosensitive two-dimensional polymeric networks comprising poly(*N*-isopropylacrylamide) chains that are mechanically interlocked by a polyglycerol platform were synthesized and characterized by different spectroscopy and microscopy methods. Encapsulation of initiator inside the pores of two-dimensional polyglycerol followed by polymerization of NIPAM resulted in a hybrid two-dimensional structure with thermosensitivity and high loading capacity properties. Thermoresponsive behavior of the synthesized material influenced the release of the loaded drugs and their biological activity. In this study, we demonstrated a new method for the polymerization of monomers inside the pores of a two-dimensional polymer to obtain a system with physically associated segments that affect the physicochemical properties of each other dramatically.

Fig. 6 Antibacterial activity measured as a function of the zone of inhibition upon incubation of **a** 2D-PNPG₃₀₀, **b** AMX/2D-PNPG₃₀₀ and **c** TC/2D-PNPG₃₀₀ at concentrations of 1) 192, 2) 96, 3) 48 μg/disc, 4) distilled water (negative control) and the middle disk) AMX and TC at a concentration of 48 μg/disc (positive control) against *E. coli* and *S. aureus* bacteria at 27 °C and 37 °C. **d** Antibacterial activity of AMX/2D-PNPG₃₀₀ against *S. aureus* upon switching temperature from 27 to 37 °C

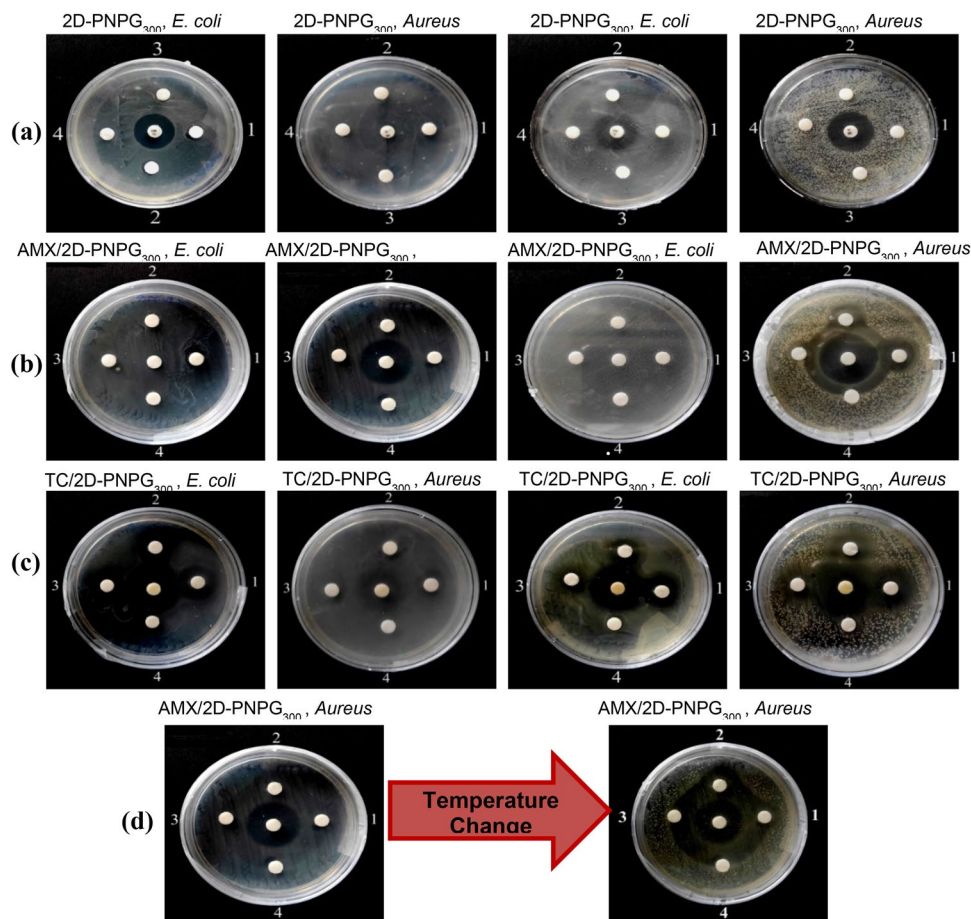


Table 3 Experimental antibacterial results of 1) AMX 2) TC 3) 2D-PNPG 4) AMX/2D-PNPG₃₀₀ 5) TC/2D-PNPG₃₀₀ at a concentration of 48 μg/disc against *E. coli* and *S. aureus*

| Antibacterial activity | | | | |
|-------------------------------|---|-------|---|-------|
| Zone of inhibition (mm) | | | | |
| Compound(48 μg/disc) | Gram-positive bacteria (<i>S. aureus</i>) | | Gram-negative bacteria (<i>E. coli</i>) | |
| | 27 °C | 37 °C | 27 °C | 37 °C |
| 1) AMX | 25 | 27 | 1 | 1 |
| 2) TC | 24 | 34 | 28 | 25 |
| 3) 2D-PNPG | 1 | 1 | 1 | 1 |
| 4) AMX/2D-PNPG ₃₀₀ | 1 | 17 | 1 | 1 |
| 5) TC/2D-PNPG ₃₀₀ | 11 | 23 | 15 | 11 |

References

- Donskyi, I.S., Azab, W., Cuellar-Camacho, J.L., Guday, G., Lippitz, A., Unger, W.E., Osterrieder, K., Adeli, M., Haag, R.: Functionalized nanographene sheets with high antiviral activity through synergistic electrostatic and hydrophobic interactions. *Nanoscale* **11**(34), 15804–15809 (2019)
- Tu, Z., Guday, G., Adeli, M., Haag, R.: Multivalent interactions between 2D nanomaterials and biointerfaces. *Adv. Mater.* **30**(33), 1706709 (2018)
- Tu, Z., Qiao, H., Yan, Y., Guday, G., Chen, W., Adeli, M., Haag, R.: Directed graphene-based nanoplateforms for hyperthermia: overcoming multiple drug resistance. *Angew. Chem.* **130**(35), 11368–11372 (2018)
- Tan, K.H., Sattari, S., Donskyi, I.S., Cuellar-Camacho, J.L., Cheng, C., Schwibbert, K., Lippitz, A., Unger, W.E., Gorbushina, A., Adeli, M.: Functionalized 2D nanomaterials with switchable binding to investigate graphene–bacteria interactions. *Nanoscale* **10**(20), 9525–9537 (2018)
- Sattari, S., Beyranvand, S., Soleimani, K., Rossoli, K., Salahi, P., Donskyi, I.S., Shams, A., Unger, W.E., Yari, A., Farjanikish, G.: Boronic acid-functionalized two-dimensional MoS₂ at biointerfaces. *Langmuir* **36**(24), 6706–6715 (2020)
- Sattari, S., Tehrani, A.D., Adeli, M., Soleimani, K., Rashidipour, M.: Fabrication of new generation of co-delivery systems based on graphene-g-cyclodextrin/chitosan nanofiber. *Int. J. Biol. Macromol.* **156**, 1126–1134 (2020)
- Beyranvand, S., Pourghobadi, Z., Sattari, S., Soleymani, K., Donskyi, I., Gharabaghi, M., Unger, W.E., Farjanikish, G., Nayebzadeh, H., Adeli, M.: Boronic acid functionalized graphene platforms for diabetic wound healing. *Carbon* **158**, 327–336 (2020)
- Bhatia, S., Donskyi, I.S., Block, S., Nie, C., Burdinski, A., Lauster, D., Radnik, J., Herrmann, A., Haag, R., Ludwig, K.: Wrapping and Blocking of influenza A viruses by sialylated 2D nanoplateforms. *Adv. Mater. Interfaces* **8**(12), 2100285 (2021)



9. Makvandi, P., Ali, G.W., Della Sala, F., Abdel-Fattah, W.I., Borzacchiello, A.: Biosynthesis and characterization of antibacterial thermosensitive hydrogels based on corn silk extract, hyaluronic acid and nanosilver for potential wound healing. *Carbohydr. Polym.* **223**, 115023 (2019)
10. Makvandi, P., Ali, G.W., Della Sala, F., Abdel-Fattah, W.I., Borzacchiello, A.: Hyaluronic acid/corn silk extract based injectable nanocomposite: a biomimetic antibacterial scaffold for bone tissue regeneration. *Mater. Sci. Eng. C* **107**, 110195 (2020)
11. Ghahremanloo, A., Zare, E.N., Salimi, F., Makvandi, P.: Electroconductive and photoactive poly (phenylenediamine)s with antioxidant and antimicrobial activities for potential photothermal therapy. *New J. Chem.* **46**(13), 6255–6266 (2022)
12. Moghaddam, F.D., Bertani, F.R.: Application of microfluidic platforms in cancer therapy. *Mater. Horiz.* **1**(1), 69–88 (2022)
13. Heidari, G., Hassanpour, M., Nejaddehbashi, F., Sarfjoo, M.R., Yousefi, S., Sharifi, E., Bigham, A., Agarwal, T., Borzacchiello, A., Lagreca, E.: Biosynthesized nanomaterials with antioxidant and antimicrobial properties. *Mater. Horiz.* **1**(1), 35–48 (2022)
14. Ghanbari, R., Khorsandi, D., Zarepour, A., Ghomi, M., Fahimi-pour, A., Tavakkoliamol, Z., Zarrabi, A.: Ionic liquid-based sensors. *Mater. Horiz.* **1**, 123–135 (2022)
15. Sattari, S., Dadkhah Tehrani, A., Adeli, M.: pH-responsive hybrid hydrogels as antibacterial and drug delivery systems. *Polymers* **10**(6), 660 (2018)
16. Zare, E.N., Zheng, X., Makvandi, P., Gheybi, H., Sartorius, R., Yiu, C.K., Adeli, M., Wu, A., Zarrabi, A., Varma, R.S.: Non-spherical metal-based nanoarchitectures: synthesis and impact of size shape, and composition on their biological activity. *Small* **17**(17), 2007073 (2021)
17. Chen, H., Jin, Y., Wang, J., Wang, Y., Jiang, W., Dai, H., Pang, S., Lei, L., Ji, J., Wang, B.: Design of smart targeted and responsive drug delivery systems with enhanced antibacterial properties. *Nanoscale* **10**(45), 20946–20962 (2018)
18. Devnarain, N., Osman, N., Fasiku, V.O., Makhathini, S., Salih, M., Ibrahim, U.H., Govender, T.: Intrinsic stimuli-responsive nanocarriers for smart drug delivery of antibacterial agents—an in-depth review of the last two decades. *Wiley Interdiscip. Rev. Nanomed. Nanobiotechnol.* **13**(1), e1664 (2021)
19. Kang, S., Park, G.H., Kim, S., Kim, J., Choi, Y., Huang, Y., Lee, Y., Choi, T.H.: Antibiotic delivery: in vitro and in vivo antimicrobial activity of antibiotic-conjugated carriers with rapid pH-responsive release kinetics. *Adv. Healthcare Mater.* **14**(2019). *Adv. Healthc. Mater.* **8**(14), 1900558 (2019)
20. Wieduwild, R., Xu, Y., Ostrovidov, S., Khademhosseini, A., Zhang, Y., Orive, G.: Engineering hydrogels beyond a hydrated network. *Adv. Healthc. Mater.* **8**(14), 1900038 (2019)
21. Sun, J., Fan, Y., Ye, W., Tian, L., Niu, S., Ming, W., Zhao, J., Ren, L.: Near-infrared light triggered photodynamic and nitric oxide synergistic antibacterial nanocomposite membrane. *Chem. Eng. J.* **417**, 128049 (2021)
22. Liu, G., Sun, X., Li, X., Wang, Z.: The bioanalytical and biomedical applications of polymer modified substrates. *Polymers* **14**(4), 826 (2022)
23. Zhang, A., Jung, K., Li, A., Liu, J., Boyer, C.: Recent advances in stimuli-responsive polymer systems for remotely controlled drug release. *Prog. Polym. Sci.* **99**, 101164 (2019)
24. Preman, N.K., Barki, R.R., Vijayan, A., Sanjeeva, S.G., Johnson, R.P.: Recent developments in stimuli-responsive polymer nanogels for drug delivery and diagnostics: a review. *Eur. J. Pharm. Biopharm.* **157**, 121–153 (2020)
25. Shi, Y., Chen, Z.: Function-driven design of stimuli-responsive polymer composites: recent progress and challenges. *J. Mater. Chem. C* **6**(44), 11817–11834 (2018)
26. Vázquez-González, M., Willner, I.: Stimuli-responsive biomolecule-based hydrogels and their applications. *Angew. Chem. Int. Ed.* **59**(36), 15342–15377 (2020)
27. Sponchioni, M., Palmiero, U.C., Moscatelli, D.: Thermo-responsive polymers: applications of smart materials in drug delivery and tissue engineering. *Mater. Sci. Eng. C* **102**, 589–605 (2019)
28. Castillo-Henríquez, L., Castro-Alpizar, J., Lopretti-Correa, M., Vega-Baudrit, J.: Exploration of bioengineered scaffolds composed of thermo-responsive polymers for drug delivery in wound healing. *Int. J. Mol. Sci.* **22**(3), 1408 (2021)
29. Arroub, K., Gessner, I., Fischer, T., Mathur, S.: Thermoresponsive poly (N-Isopropylacrylamide)/polycaprolacton nanofibrous scaffolds for controlled release of antibiotics. *Adv. Eng. Mater.* **23**(9), 2100221 (2021)
30. Bahara, P., Hassania, A.H., Panahib, H.A., Moniric, E.: Application of modified graphene oxide with thermosensitive polymers for adsorption of antibiotics from synthetic contaminated water. *Desalin. Water Treat.* **210**, 281–295 (2021)
31. Schultz, H.B., Vasani, R.B., Holmes, A.M., Roberts, M.S., Voelcker, N.H.: Stimulus-responsive antibiotic releasing systems for the treatment of wound infections. *ACS Appl. Bio Mater.* **2**(2), 704–716 (2019)
32. Tan, K.H., Sattari, S., Beyranvand, S., Faghani, A., Ludwig, K., Schwibbert, K., Böttcher, C., Haag, R., Adeli, M.: Thermoresponsive amphiphilic functionalization of thermally reduced graphene oxide to study graphene/bacteria hydrophobic interactions. *Langmuir* **35**(13), 4736–4746 (2019)
33. Jiang, R., Yi, Y., Hao, L., Chen, Y., Tian, L., Dou, H., Zhao, J., Ming, W., Ren, L.: Thermoresponsive nanostructures: from mechano-bactericidal action to bacteria release. *ACS Appl. Mater. Interfaces.* **13**(51), 60865–60877 (2021)
34. Bruk, L.A., Dunkelberger, K.E., Khampang, P., Hong, W., Sadagopan, S., Alper, C.M., Fedorchak, M.V.: Controlled release of ciprofloxacin and ceftriaxone from a single ototopical administration of antibiotic-loaded polymer microspheres and thermoresponsive gel. *PLoS ONE* **15**(10), e0240535 (2020)
35. Cao, M., Wang, Y., Hu, X., Gong, H., Li, R., Cox, H., Zhang, J., Waigh, T.A., Xu, H., Lu, J.R.: Reversible thermoresponsive peptide–PNIPAM hydrogels for controlled drug delivery. *Biomacromol* **20**(9), 3601–3610 (2019)
36. Deirram, N., Zhang, C., Kermaniyan, S.S., Johnston, A.P., Such, G.K.: pH-responsive polymer nanoparticles for drug delivery. *Macromol. Rapid Commun.* **40**(10), 1800917 (2019)
37. Tu, Z., Wycisk, V., Cheng, C., Chen, W., Adeli, M., Haag, R.: Functionalized graphene sheets for intracellular controlled release of therapeutic agents. *Nanoscale* **9**(47), 18931–18939 (2017)
38. Tu, Z., Achazi, K., Schulz, A., Mülhaupt, R., Thierbach, S., Rühl, E., Adeli, M., Haag, R.: Combination of surface charge and size controls the cellular uptake of functionalized graphene sheets. *Adv. Funct. Mater.* **27**(33), 1701837 (2017)
39. Sattari, S., Adeli, M., Beyranvand, S., Nemat, M.: Functionalized graphene platforms for anticancer drug delivery. *Int. J. Nanomed.* **16**, 5955 (2021)
40. Nikfarjam, N., Ghomi, M., Agarwal, T., Hassanpour, M., Sharifi, E., Khorsandi, D., Khan, M.A., Rossi, F., Rossetti, A., Zare, E.N.: Antimicrobial ionic liquid-based materials for biomedical applications. *Adv. Funct. Mater.* **42**(2021). *Adv. Funct. Mater.* **31**(42), 2170312 (2021)
41. Faghani, A., Donskyi, I.S., Fardin Gholami, M., Ziem, B., Lip-pitz, A., Unger, W.E., Böttcher, C., Rabe, J.P., Haag, R., Adeli, M.: Controlled covalent functionalization of thermally reduced graphene oxide to generate defined bifunctional 2D nanomaterials. *Angew. Chem.* **129**(10), 2719–2723 (2017)
42. Donskyi, I.S., Nie, C., Ludwig, K., Trimpert, J., Ahmed, R., Quaa, E., Achazi, K., Radnik, J., Adeli, M., Haag, R.: Graphene

- sheets with defined dual functionalities for the strong SARS-CoV-2 interactions. *Small* **17**(11), 2007091 (2021)
43. Gholami, M.F., Lauster, D., Ludwig, K., Storm, J., Ziem, B., Severin, N., Böttcher, C., Rabe, J.P., Herrmann, A., Adeli, M.: Functionalized graphene as extracellular matrix mimics: toward well-defined 2D nanomaterials for multivalent virus interactions. *Adv. Funct. Mater.* **27**(15), 1606477 (2017)
44. Mohammadifar, E., Ahmadi, V., Gholami, M.F., Oehrl, A., Kolyvushko, O., Nie, C., Donskyi, I.S., Herziger, S., Radnik, J., Ludwig, K.: Graphene-assisted synthesis of 2D polyglycerols as innovative platforms for multivalent virus interactions. *Adv. Funct. Mater.* **31**(22), 2009003 (2021)
45. Lan, J., Ge, J., Yu, J., Shan, S., Zhou, H., Fan, S., Zhang, Q., Shi, X., Wang, Q., Zhang, L.: Structure of the SARS-CoV-2 spike receptor-binding domain bound to the ACE2 receptor. *Nature* **581**(7807), 215–220 (2020)
46. Clausen, T.M., Sandoval, D.R., Spliid, C.B., Pihl, J., Perrett, H.R., Painter, C.D., Narayanan, A., Majowicz, S.A., Kwong, E.M., McVicar, R.N.: SARS-CoV-2 infection depends on cellular heparan sulfate and ACE2. *Cell* **183**(4), 1043–1057 (2020)
47. Ahmadi, V., Nie, C., Mohammadifar, E., Achazi, K., Wedepohl, S., Kerkhoff, Y., Block, S., Osterrieder, K., Haag, R.: One-pot gram-scale synthesis of virucidal heparin-mimicking polymers as HSV-1 inhibitors. *Chem. Commun.* **57**(90), 11948–11951 (2021)
48. Zheng, Y., Hong, X., Wang, J., Feng, L., Fan, T., Guo, R., Zhang, H.: 2D nanomaterials for tissue engineering and regenerative nanomedicines: recent advances and future challenges. *Adv. Healthc. Mater.* **10**(7), 2001743 (2021)

Publisher's Note Springer Nature remains neutral with regard to jurisdictional claims in published maps and institutional affiliations.

Springer Nature or its licensor holds exclusive rights to this article under a publishing agreement with the author(s) or other rightsholder(s); author self-archiving of the accepted manuscript version of this article is solely governed by the terms of such publishing agreement and applicable law.

